An Evanescent-mode Tunable Dual-band Filter with Independently-Controlled Center Frequencies

***Abstract*—This paper presents a novel design of a highly tunable dual-band bandpass filter based on evanescent-mode cavity resonators with two capacitive loadings which results in two independently tunable resonant frequencies. High unloaded quality factor, for both resonant modes, and small filter size is achieved since the two modes share the same physical volume of a single cavity. In addition, the internal and external couplings of the filter can be controlled independently at the two passbands to create flexible frequency responses. An example design of the proposed filter is prototyped in a substrate-integrated fashion and demonstrates: 1) a first tunable passband of 1.156–1.741 GHz with 3-dB bandwidth (BW) of 76–156 MHz and insertion loss (IL) of 3.13–1.109 dB, and 2) a second passband of 2.242–3.648 GHz with 3-dB BW of 125–553 MHz and IL of 7.551–1.299 dB.**

***Index Terms*—dual-band filters, tunable filters, evanescent-mode filters**

I. Introduction

Interference mitigation is a critical concern for future multi-band multi-frequency high-frequency communication and sensing systems. Compared to a bank of fixed frequency filters, electronic tunable/reconfigurable bandpass and band-stop filters provide more flexible frequency responses and potentially reduced complexity/loss in signal routing. Dual- and triple-band tunable bandpass filters offer selectivity for multiple signal frequencies concurrently.

Several tunable dual-band bandpass filter designs have been reported in recent years [1]–[5]. Conventionally, dual-band filters are designed by parallel integration of two band-pass filters using duplexing elements, cascading a band-stop filter with a band-pass filter, direct synthesis, and utilization of the even and odd modes of transmission line resonators. The reported dual-band filters are predominantly based on various forms of microstrip line resonators. Although compact in size, such dual-band filters suffer from relatively low unloaded quality factor.

In this paper, we present a novel tunable dual-band filter design methodology based on evanescent-mode cavity resonators with two capacitive loadings. Fig. 1 shows an illustration of a 2-pole tunable dual-band filter consisting of two of such resonators. Each resonator consists of a cavity and two conductive posts, both connected to the resonator on one end. On the end, the posts are connected to the cavity through varactors whose capacitance can be electronically changed by the reverse bias voltage. Similar to a capacitively loaded coaxial resonator, the first two resonant frequencies of the proposed cavity resonator can be tuned by the loading capacitance and are relatively independent of each other, thus making it possible to design dual-band filters with flexible passband frequencies. Input/output coupling is provided by coplanar waveguides

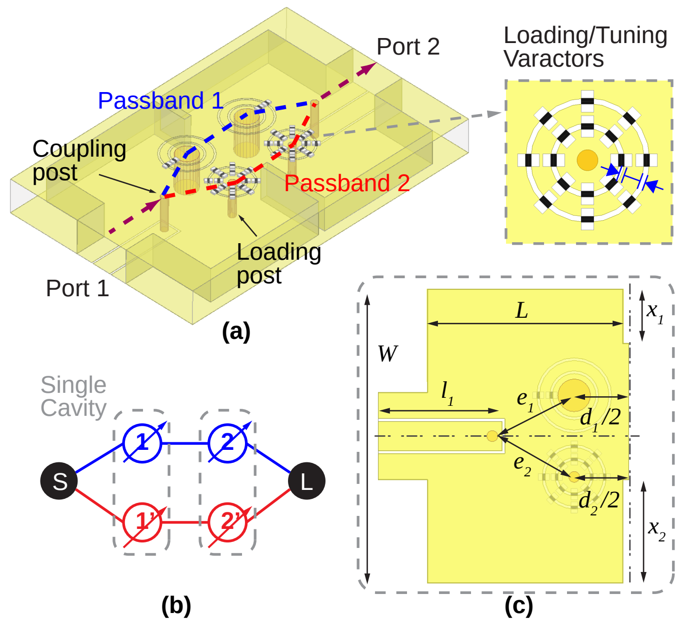

Fig. 1. (a) Concept of the proposed tunable dual-band filter. The inset shows the capacitive loading and tuning scheme using reversed connected varactors. (b) Signal routing diagram of the filter. (c) Top view of one of the resonators with critical dimensions labeled.

shorted to the cavity by vias. The inter-resonator and external coupling coefficients of the two passbands can be controlled relatively independently by the placement of the loading posts and the input/output coupling structures.

II. Design

A. Resonator Design

Fig. 2 presents the simulated electric field patterns and the resonant frequencies f_1 and f_2 of an example of the proposed resonator. The length of the resonator is 18 mm and the width is 27 mm. It is clear from the field distribution plot (Fig. 2-a&b) that when one loading post is at resonance, the other one does not introduce significant perturbation to the field pattern. This is confirmed by the resonant frequency plot in Fig. 2-c&d which shows that the tuning of one resonance has negligible effect on the other.

B. 2-pole Filter Design

A 2-pole tunable dual-band filter is designed, using the above-mentioned resonators, in order to demonstrate the design concept. The inter-resonator coupling between the two resonators is achieved by magnetic coupling through an open window in the resonator sidewall. The coupling coefficient (k_c) dependents on a few parameters, such as the window width

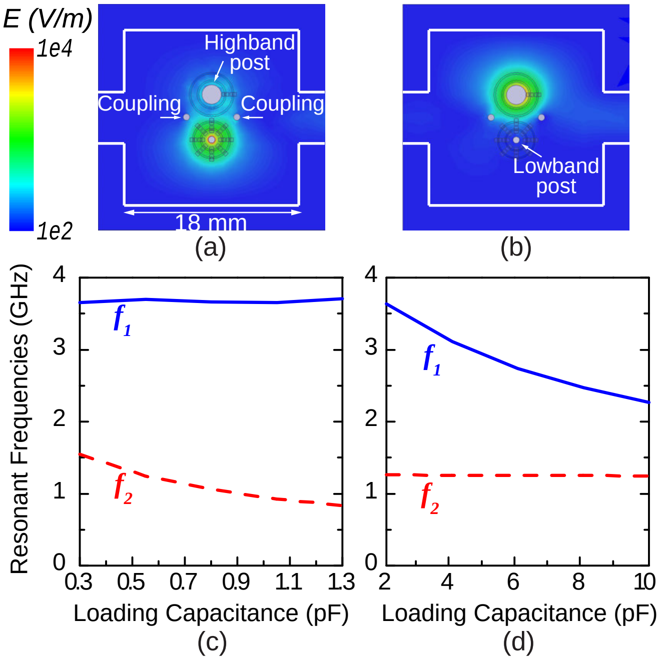

Fig. 2. Simulated field distribution of (a) the lowband resonance and (b) the highband resonance. Simulated resonant frequency change for (c) the lowband tuning and (d) the highband tuning.

and the positions of the capacitive posts. A wider window opening generally gives higher coupling coefficients for both bands. Coupling is also stronger when the two posts are closer to the coupling window. Fig. 3 shows the simulated coupling coefficients k_{c1} and k_{c2} of the two bands with respect to the window width x_1 and x_2 (fixed post separation of $d = d_1 = d_2 = 10$ mm is assumed). When x_1 is swept, x_2 is kept at 9.5 mm, and when x_2 is swept, x_1 is kept at 5 mm. It can be observed that k_{c1} (highband) changes from 0.11 to 0.03 when x_1 changes from 0.5 mm to 8 mm, whereas k_{c2} exhibits less relative change or from 0.06 to 0.035.

The external coupling is achieved by magnetic coupling between the input/output coupling posts and the capacitive posts (Fig. 1-a). In general, the coupling strength is directly related to the distance (e_1 and e_2) between the coupling post and the capacitive posts. In order to achieve individual control of the external coupling, one can use the following, intuitive procedure: 1) the external coupling of the lower band can be determined by choosing a proper value for e_1, 2) the coupling post can then be moved along an equi-distance circle around the lowband loading post until the required external coupling to the highband post is achieved. In practice, a few iterations may be needed to optimize the design.

This procedure requires that both the $x-$ and $y-$ coordinates of the coupling posts need to be adjusted. Due to the page limit of this abstract, we present design data for only when the $x-$coordinates of the coupling posts are adjusted. Fig. 4 shows the simulated external quality factor (Q_e) for the two bands with respect to the length of the CPW feedlines.

Using the described procedure a 2-pole dual-band bandpass filter is designed as a proof of concept. All filter simulations

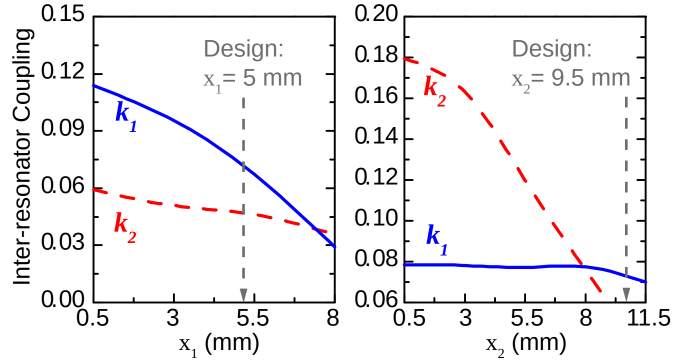

Fig. 3. Simulated inter-resonator coupling coefficients as a function of the wall sizes that form the inductive iris, along with the chosen values for the presented filter design.

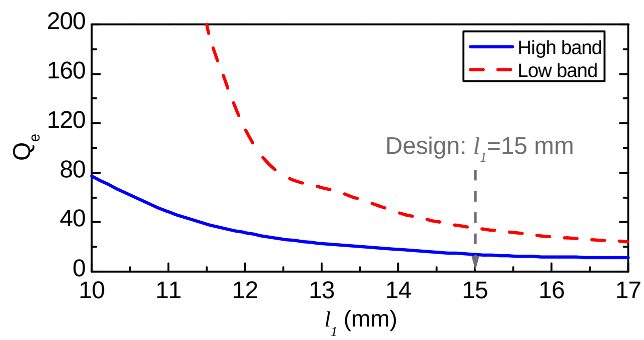

Fig. 4. External coupling coefficient for both modes as a function of the RF feedline length, along with the chosen value for the presented filter design.

are performed using ANSYS HFSS and the results are shown in Fig. 5. Due to the frequency separation between the two passbands, two simulations with different solution frequencies are required for each tuning configuration: one for the highband, which includes the wide frequency span; and one specifically for the lowband. This ensures proper convergence of both passbands. The insets in Fig. 5 show the detailed lowband response.

III. Experimental Validation

The proposed filter is fabricated in a substrate-integrated fashion using a 5-mm-thick Roger TMM-3 laminate with double side copper cladding. The loading posts and the input/output coupling posts are drilled vias of the desired sizes. Electroplating is used to fill the vias with copper. Subsequently, the coplanar waveguide feed lines are defined using a milling machine. Skyworks SMV1405-040LF varactors are surface mounted across the double ring gaps so that they can be reverse connected for better linearity. Biasing is done through a 750-kΩ resistor as an RF choke. Fig. 6 shows the fabricated filter.

Measurement of the filter responses is taken with a vector network analyzer (VNA) at the various bias voltages. Fig. 7 shows the tuning characteristics of the lower passband and the higher passband. The lower band has a tuning range of 1.156–1.741 GHz with a bandwidth of 76–156 MHz and an insertion loss (IL) of 3.13–1.109 dB. The higher band has a

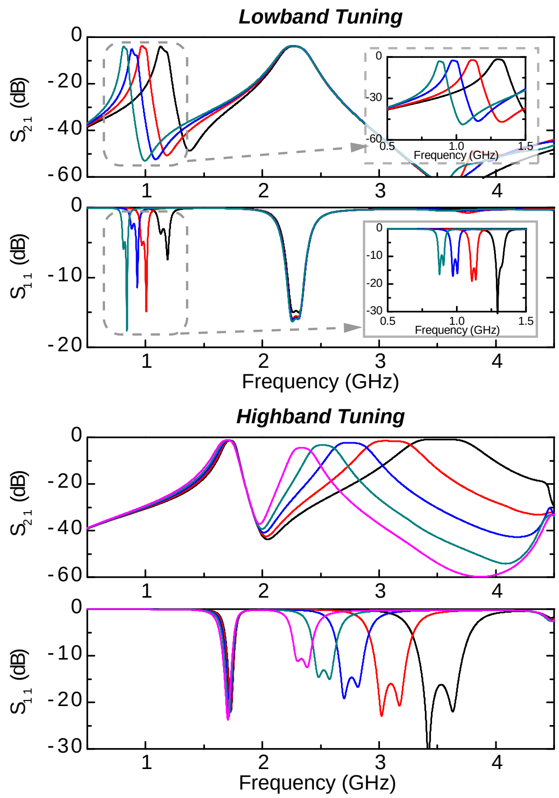

Fig. 5. Simulated tuning performance of the proposed tunable dual-band filter. The insets show the S-parameters from the narrow band simulation for the lowband passband.

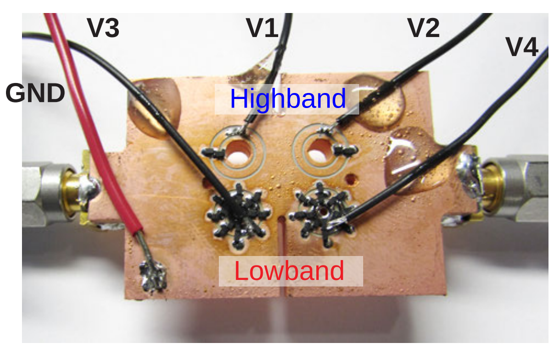

Fig. 6. Photograph of the fabricated tunable dual-band filter.

tuning range of 2.242–3.648 GHz with a bandwidth of 125–553 MHz and an IL of 7.551–1.299 dB. Overall, the measured performance of the filter agrees very well with the simulation results (Fig. 5).

It is clear from the measurement that the tuning of one of the bands has minimal effect on the other. One exception is when the two bands are tuned to very close to each other (Fig. 7-a&c) where the roll-off of the lowband filter causes a noticeable reduction of the bandwidth of the highband. The minimum separation that can be allowed between the two bands is determined by the filter shape factors of the two passbands. In general, the sharper the roll-off, the smaller the separation.

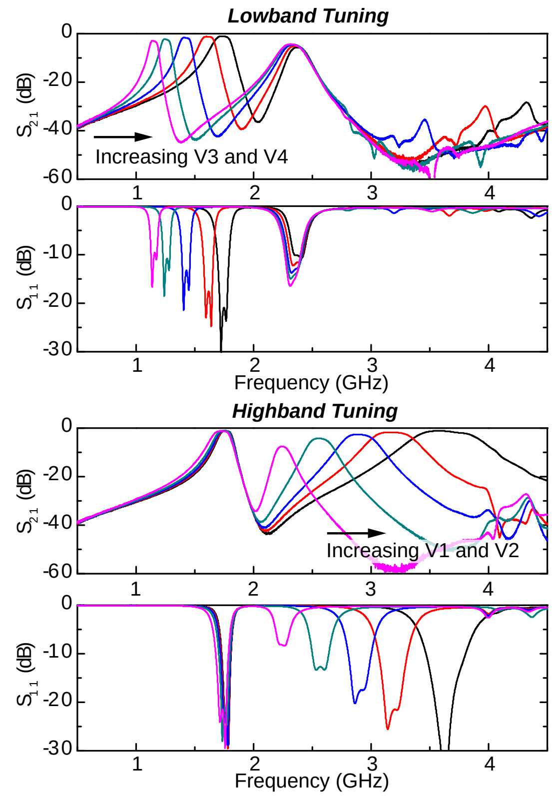

Fig. 7. Measured performance of the fabricated tunable dual-band filter.

IV. Conclusion

A new tunable dual-band bandpass filter with independent frequency control of each passband is presented. The filter is realized using substrate-integrated, evanescent-mode, cavity filters loaded with commercially available varactor diodes. Dual-band operation is demonstrated with tunable passbands ranging from 1.156–1.741 GHz and 2.242–3.648 GHz, for the lowband and highband, respectively. This implementation results in a compact and low-loss dual-band bandpass filter design that can be integrated in reconfigurable front-end hardware for the next generation of adaptable and cognitive radios.

References

[1] B. You, L. Chen, Y. Liang, and X. Wen, "A High-Selectivity Tunable Dual-Band Bandpass Filter Using Stub-Loaded Stepped-Impedance Resonators," *IEEE Microwave and Wireless Components Letters*, vol. 24, no. 11, pp. 736–738, Nov. 2014.

[2] X. Huang, L. Zhu, Q. Feng, Q. Xiang, and D. Jia, "Tunable bandpass filter with independently controllable dual passbands," *IEEE Transactions on Microwave Theory and Techniques*, vol. 61, no. 9, pp. 3200–3208, Sept. 2013.

[3] T. Yang and G. Rebeiz, "Three-pole 1.3–2.4-GHz diplexer and 1.1–2.45-GHz dual-band filter with common resonator topology and flexible tuning capabilities," *IEEE Transactions on Microwave Theory and Techniques*, vol. 61, no. 10, pp. 3613–3624, 2013.

[4] G. Chaudhary, Y. Jeong, and J. Lim, "Harmonic suppressed dual-band bandpass filters with tunable passbands," *IEEE Transactions on Microwave Theory and Techniques*, vol. 60, no. 7, pp. 2115–2123, Jul. 2012.

[5] D. Girbau, A. Lazaro, A. Perez, E. Martinez, L. Pradell, and R. Villarino, "Tunable dual-band filters based on capacitiveloaded stepped-impedance resonators," in *Proceedings of the 39th European Microwave Conference*, 2009.